J Bioenerg Biomembr (2009) 41:299–308
DOI 10.1007/s10863-009-9228-4

Mitochondrial bioenergetics and redox state are unaltered in *Trypanosoma cruzi* isolates with compromised mitochondrial complex I subunit genes

Julio César Carranza · Alicia J. Kowaltowski · Marco Aurélio G. Mendonça · Thays C. de Oliveira · Fernanda R. Gadelha · Bianca Zingales

Received: 10 June 2009 / Accepted: 15 June 2009 / Published online: 18 July 2009

Abstract In trypanosomatids the involvement of mitochondrial complex I in NADH oxidation has long been debated. Here, we took advantage of natural *Trypanosoma cruzi* mutants which present conspicuous deletions in *ND4*, *ND5* and *ND7* genes coding for complex I subunits to further investigate its functionality. Mitochondrial bioenergetics of wild type and complex I mutants showed no significant differences in oxygen consumption or respiratory control ratios in the presence of NADH-linked substrates or $FADH_2$-generating succinate. No correlation could be established between mitochondrial membrane potentials and *ND* deletions. Since release of reactive oxygen species occurs at complex I, we measured mitochondrial H_2O_2 formation induced by different substrates. Significant differences not associated to *ND* deletions were observed among the parasite isolates, demonstrating that these mutations are not important for the control of oxidant production. Our data support the notion that complex I has a limited function in *T. cruzi*.

Keywords Mitochondrial complex I · Complex I subunits · NADH oxidation · Fumarate reductase · Hydrogen peroxide mitochondrial production · Mitochondrial membrane potential

Abbreviations

CCCP	carbonylcyanide m-chlorophenylhydrazone
$DiOC_6(3)$	3,3′-dihexyloxacarbocyanine iodide
FRD	NADH-dependent fumarate reductase
HRP	horseradish peroxidase
kDNA	kinetoplast DNA
LIT	liver infusion tryptose
ND	complex I subunits
PBS	phosphate-buffered saline
PPP	pentose phosphate pathway
RCR	respiratory control ratio
ROS	reactive oxygen species
SRM	standard intracellular reaction medium
Wt	wild type

Introduction

The protozoan parasite *Trypanosoma cruzi* is the etiological agent of Chagas disease, which afflicts 16 million people in Latin American countries. Chagas disease has a range of clinical manifestations, from asymptomatic to severe cardiac and digestive forms. Both host and parasite genetics play roles in the disease state (reviewed by Campbell et al. 2004).

T. cruzi belongs to the protozoan Kinetoplastida order, characterized by the presence of a single mitochondrion

J. César Carranza · A. J. Kowaltowski · B. Zingales (✉)
Departamento de Bioquímica, Instituto de Química,
Universidade de São Paulo,
Avenida Professor Lineu Prestes, 748 CEP 05508-000,
São Paulo, SP, Brasil
e-mail: zingales@iq.usp.br

M. A. G. Mendonça · T. C. de Oliveira · F. R. Gadelha
Departamento de Bioquímica, Instituto de Biologia,
Universidade Estadual de Campinas,
Campinas, SP, Brasil

Present Address:
J. César Carranza
Laboratorio de Investigaciones en Parasitología Tropical,
Facultad de Ciencias, Universidad del Tolima,
A.A. No. 546,
Ibagué, Colombia

branching throughout the cell. Inside this organelle, a specialized region, named kinetoplast, concentrates mitochondrial DNA (kDNA), that accounts for 20–30% of the total cellular DNA. kDNA is a dense network composed by 20–50 maxicircles and thousands of minicircles. Maxicircles are the functional equivalent of mitochondrial DNA of other eukaryotes, containing genes for mitochondrial 9S and 12S ribosomal RNA, subunits I, II and III of the cytochrome c oxidase, seven subunits of complex I (see below), subunit 6 of the ATP synthase, apocytochrome b, ribosomal protein S12 and several genes with unknown function (Simpson et al. 1987). To become operative, transcripts of most of these genes must undergo a specific type of processing, termed RNA editing, which involves additions and, less frequently, deletions of uridylate residues. Information for editing resides in small transcripts, named guide RNAs, which are mainly encoded by minicircles (reviewed by Stuart et al. 2002).

The intermediate metabolism of *T. cruzi* has been extensively studied (reviewed by Cazzulo 1994; Bringaud et al. 2006). Most metabolic studies were performed with axenic culture epimastigotes, showing that this stage is able to consume both carbohydrates and amino acids, although glucose is preferred and consumed first when both are present (Cannata and Cazzulo 1984). In most trypanosomatids, succinate is the major end product of glucose metabolism. This substrate is produced both in the glycosome, an organelle unique to kinetoplastids that contains most of the glycolytic enzymes, and in the mitochondrion by NADH-dependent fumarate reductases (FRD). These enzymes oxidize NADH and generate succinate (Boveris et al. 1986; Besteiro et al. 2002; Coustou et al. 2005; Coustou et al. 2006). The production of succinate and its excretion, which probably occurs when the respiratory chain is not able to deal with the input of reduction equivalents, has been attributed to the fact that the *T. cruzi* respiratory chain is adapted to the oxidation of succinate through complex II, instead of NADH.

In trypanosomatids, the presence of an electron transport from complex II to complex IV has been demonstrated, but several arguments have been made against a significant contribution of complex I (NADH:ubiquinone oxidoreductase) to energy metabolism (reviewed by Opperdoes and Michels 2008). Indeed, NADH-dependent substrates are not able to stimulate ATP production in isolated mitochondria (Turrens 1989) and reduction of cytochrome c by NADH-dependent substrates is insensitive to antimycin A, suggesting that the electrons from NADH do not reach cytochrome c via complex III (Turrens 1989; Denicola-Seoane et al. 1992). An alternative rotenone-insensitive NADH dehydrogenase, also called type-II NADH dehydrogenase, was described in *T. brucei* procyclic forms (Fang and Beattie 2002). This enzyme, located in the inner mitochondrial membrane, oxidizes NADH and transfers electrons to ubiquinone.

Although the functionality of complex I in trypanosomatids has long been debated, the complete architecture of complex I in these organisms was recently elucidated showing that it has at least 19 subunits and a minimum mass of ~660 kDa (Opperdoes and Michels 2008) (Fig. 1). All subunits known to be involved in electron transfer are present, but four membrane subunits encoded by the eukaryotic mitochondrial genome, and supposedly involved in proton extrusion are missing.

T. cruzi strains show substantial heterogeneity in biological and biochemical characteristics, which are resultant from a high genetic diversity (reviewed by Campbell et al. 2004). The maxicircle genomes of two *T. cruzi* strains, CL Brener and Esmeraldo, were assembled and annotated from data generated by the *T. cruzi* Sequencing Consortium (Westenberger et al. 2006). In the coding region, strain-specific insertions and deletions in particular genes were reported. As in other trypanosomatids, the maxicircle genome encodes seven complex I subunits: ND1, ND3-ND5, and ND7-ND9. The Esmeraldo strain contains a unique 236-bp deletion that removes the 5′-ends of *ND4* and *CR4* genes and the intergenic region (Westenberger et al. 2006). Additionally, the Esmeraldo *ND5* gene has three frameshift mutations relative to the CL Brener sequence, which would generate a truncated protein of 165 amino acids as compared to the 589 amino acid product of CL Brener (Westenberger et al. 2006). In previous studies, we showed that the *ND7* gene of some *T. cruzi* isolates presents a conserved 455-bp deletion in the center of the coding region relative to wild type (Wt) *ND7* gene (755 bp) of the CL Brener strain (Baptista et al. 2006; Carranza et al. 2009). Such a large deletion should impair the functionality of the ND7 subunit.

In the present study, we took advantage of natural mutants of *T. cruzi*, which present conspicuous deletions in the *ND4*, *ND5* and *ND7* genes coding for complex I subunits (see localization of the subunits in Fig. 1), to

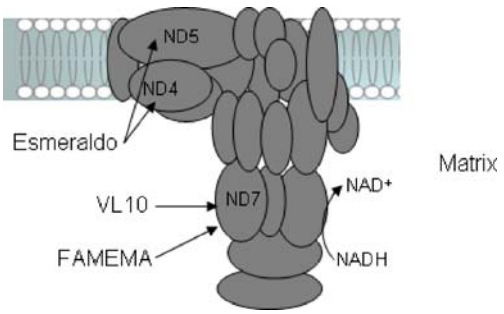

Fig. 1 Schematic of trypanosomatid mitochondrial complex I, where only some subunits are depicted (adapted from Opperdoes and Michels 2008). The positions of the ND4, ND5 and ND7 subunits and the *T. cruzi* isolates bearing *ND* mutations are shown

further investigate the functionality of this complex in the oxidation of NADH, generation of mitochondrial reactive oxygen species (ROS) and mitochondrial membrane potential. Our data support evidence that complex I has a limited function in *T. cruzi* and that a considerable fraction of mitochondrial NADH is oxidized by FRD. Our data also demonstrate that these deletions have no consequence on mitochondrial bioenergetics or redox state.

Materials and methods

Parasite isolates and culture conditions

The characteristics of *T. cruzi* isolates employed in this study are described in Table 1. Epimastigote forms were cultured in liver infusion tryptose (LIT) medium containing 20 mg/L hemin and 10% fetal calf serum, at 28°C (Castellani et al. 1967). In the log phase, parasites were collected by centrifugation (1,000 g, 4°C, 5 min), washed and ressuspended in phosphate-buffered saline (PBS). The number of parasites was estimated in a Newbauer chamber. Protein concentration was determined by the Bradford method (Bradford 1976).

Structure of *ND7* and *ND4* genes

The structure of the *ND7* and *ND4* genes was established by PCR amplification as previously reported (Baptista et al. 2006; Carranza et al. 2009). PCR products of were separated in 0.8% agarose gels and stained with ethidium bromide.

Oxygen consumption measurements

Oxygen consumption was monitored using a computer-interfaced Clark-type electrode operating with continuous stirring, at 28°C. Cells (5×10^7 cells/mL) were incubated in a standard intracellular reaction medium (SRM) containing 125 mM sucrose; 65 mM KCl; 10 mM Hepes pH 7.2; 1 mM $MgCl_2$; 2 mM KH_2PO_4 and 0.5 mM EGTA, in the presence of 64 μM digitonin and the respiratory substrates: 5 mM malate/5 mM pyruvate (complex I-linked substrates) or 5 mM succinate (a complex II-linked substrate). ADP (200 μM) and oligomycin (1 μg/mL) were added to achieve state 3 and 4 respiratory rates, respectively. In some experiments, malonate (10 mM) was employed to inhibit complex II. Respiratory control ratios (RCR, state 3/state 4) were determined.

Mitochondrial membrane potential ($\Delta\Psi$) measurements in intact cells

Epimastigotes (10^6 cells/mL) were incubated in SRM in the presence of 0.3 nM 3,3′-dihexyloxacarbocyanine iodide dye ($DiOC_6(3)$) (Srivastava et al. 1997; Campos et al. 2004) for 40 min at 28°C. Carbonylcyanide m-chlorophenylhydrazone (CCCP) 1 μM was added to one of the tubes and after a further incubation for 20 min the cells were analyzed in a FACSCalibur flow cytometer (Becton Dickinson). The F/F_{CCCP} ratio was used to normalize the results, where F is the mean fluorescence intensity of the probe (F max) and F_{CCCP} is the mean fluorescence in the presence of CCCP (F min).

Hydrogen peroxide (H_2O_2) release measurements

Epimastigotes (5×10^7 cells/mL) were incubated in SRM containing 64 μM digitonin, 50 μM Amplex red (Molecular Probes) (Zhou et al. 1997), 1 U/mL HRP and 5 mM pyruvate/5 mM malate (complex I) or 5 mM succinate (complex II). Fluorescence was followed in a temperature controlled Hitachi F-4500 fluorescence spectrophotometer operating at excitation and emission wavelengths of 563 and 587 nm, respectively, with continuous stirring. Data were calibrated by adding known quantities of a freshly prepared H_2O_2 (Kowaltowski et al. 2004).

NAD(P) levels

The levels of mitochondrial NAD(P)H were monitored by recording reduced pyridine nucleotide fluorescence intensity (λex=352 nm, λem=464 nm) (Mayevsky and Rogatsky 2007) at 28°C using a Hitachi F-4500 fluorescence spectrometer equipped with magnetic stirring. Epimasti-

Table 1 Characteristics of *T. cruzi* isolates used in this study

Isolate	Host	Structure of complex I genes[a]	
		ND7	*ND4*
CL Brener	*Triatoma infestans*	Wt	Wt
Esmeraldo[b]	Human; acute phase	Wt	Δ
115	Human; chronic phase; cardiac form	Wt	Wt
VL10	Human; chronic phase; indeterminate form	Δ	Wt
FAMEMA	Human; chronic phase; indeterminate form	Δ	Wt

[a] The structure of *ND7* and *ND4* genes was determined by PCR assays

[b] Also presents *ND5* frameshift mutations (Westenberger et al. 2006)

Wt, wild type; Δ, deletion

gotes (5×10^7 cells/mL) were ressuspended in SRM and after basal measurements, antimycin A (0.5 μg/mL) or CCCP (1 μM) were added. $NAD(P)^+$ concentrations were estimated by the difference between F_2 (maximal accumulation of NAD(P)H upon addition of antimycin A) and F_1 (basal fluorescence). The relative concentration of NAD(P)H was determined by the difference between F1 and F3 (maximal oxidation promoted by the addition of CCCP). The variation in the concentration of total NAD(P) was obtained by the difference between F2 and F3. A calibration curve constructed with known concentrations of NADH established that 1 μM NADH corresponds to 23.65 fluorescence arbitrary units.

Susceptibility to hydrogen peroxide

Parasites (2.4×10^7 cells/mL) were incubated in PBS in the presence of different concentrations of H_2O_2 (40–160 μM) for 1 h at 28°C (Mielniczki-Pereira et al. 2007). Then cells were centrifuged (1,000 g, 7 min, 4°C), ressuspended in LIT medium and after 24 h of growth at 28°C, the number of parasites was determined in a Neubauer chamber. The H_2O_2 concentration that promoted 50% inhibition of parasite proliferation (IC_{50}) was calculated using Origin Pro 7.0 software. H_2O_2 concentration in stock solutions was determined at 230 nm before each experiment using an extinction coefficient of 81 $M^{-1}cm^{-1}$.

NADPH production by the pentose phosphate pathway (PPP)

Cells (10^8 cells/mL) were incubated at 28°C in a reaction medium containing 50 mM Tris–HCl, pH 7.6; 50 mM KCl; 0.1% Triton X-100; 80 μM leupeptin; 250 μM $NADP^+$; 2 mM $MgCl_2$; 1 mM 6-phosphogluconate and 1 mM glucose-6-phosphate. The time course of $NADP^+$ reduction was followed at 340 nm (Mielniczki-Pereira et al. 2007).

Statistical analysis

Data shown represent either averages±standard errors or representative traces of at least three experiments conducted with different cell preparations. Comparisons were conducted using Student′s *t*-test, with Origin 7.0 software, and $p<0.05$ was considered significant.

Results

Characteristics of *T. cruzi* isolates

In this study, we used *T. cruzi* isolates originating from different Brazilian states (Table 1). Four isolates were obtained from human patients and one (CL Brener) from the insect vector *Triatoma infestans*. The structure of the *ND7* and *ND4* mitochondrial genes was determined using the PCR assays previously described (Baptista et al. 2006; Carranza et al. 2009). The sensitivity of these assays allows the conclusion that in a particular strain all the copies of the genes under analysis are wild type (Wt) or present deletions (Δ). Accordingly, the CL Brener, Esmeraldo and 115 isolates present the Wt *ND7* gene, whereas VL10 and FAMEMA show a conserved 455-bp deletion. Only the Esmeraldo isolate contains a deletion in *ND4* (Westenberger et al 2006). The *ND5* gene of this strain has frameshift mutations that originate a truncated protein (Westenberger et al 2006). In the present study we have not determined whether the *ND5* gene of the 115, VL10 and FAMEMA strains also bears these mutations. The location of the referred complex I subunits is shown in Fig. 1. ND5 (71 kDa) and ND4 (52 kDa) subunits participate in the transmembrane domain imbedded in the inner mitochondrial membrane, whereas the ND7 subunit (45 kDa) is predicted to be an iron-sulfur protein, localized in the hydrophilic domain inside the mitochondrial matrix.

Oxygen consumption and respiratory control

The presence of a single mitochondrion in trypanosomatids has hampered the isolation of coupled mitochondria for studies of energy linked functions of these organelles. Nevertheless, digitonin permits the selective permeabilization of *T. cruzi* plasma membrane without affecting the functional integrity of mitochondria (Vercesi et al 1991). To establish to optimal digitonin concentration for the selective permeabilization of the epimastigote cell membrane, we initially measured oxygen consumption in intact cells using a Clark-type electrode and verified that it was not altered upon addition of 200 μM ADP and/or 5 mM succinate (data not shown). Next, the respiratory control ratio (RCR) on addition of succinate was determined in the presence of increasing concentrations of digitonin. A progressive increment of RCRs was recorded up to a digitonin concentration of 64 μM. Further increases of the detergent promoted a decrease of RCR values. Accordingly, we adopted 64 μM digitonin for further studies, since under this condition respiration and phosphorylation were coupled.

To verify whether the mutations in the *ND7*, *ND4* or *ND5* genes affect mitochondrial respiration, we measured oxygen consumption in digitonin-permeabilized epimastigotes in the presence of NADH-linked mitochondrial substrates (pyruvate and malate) and $FADH_2$-generating succinate (Table 2). All substrates stimulated oxygen consumption and no significant differences in respiratory rates were observed among the isolates using either substrate, although pyruvate/malate supported-respiratory rates were higher than those

Table 2 Oxygen consumption rates and respiratory control ratios in *T. cruzi* isolates in the presence of complex I and complex II substrates

	Wt *ND7*			Δ *ND7*	
	CL Brener	Esmeraldo[a]	115	VL10	FAMEMA
Complex I substrates (pyruvate/malate)					
Respiratory rates (nmol O_2 . mg cell protein^{-1} . min^{-1})					
State 3	4.86±0.8	4.14±0.24	4.22±0.27	4.59±0.4	4.5±0.75
State 4	2.12±0.74	1.9±0.07	1.99±0.15	1.96±0.45	1.85±0.27
Respiratory control ratios (State 3/State 4)					
	2.29±0.4	2.17±0.07	2.12±0.2	2.34±0.34	2.43±0.33
Complex II substrate (succinate)					
Respiratory rates (nmols O_2 . mg cell protein^{-1} . min^{-1})					
State 3	4.35±0.35	3.99±0.26	4.36±0.9	3.76±0.46	3.55±0.8
State 4	1.98±0.56	2.04±0.2	1.59±0.24	1.75±0.45	1.63±0.07
Respiratory control ratios (State 3/State 4)					
	2.2±0.69	1.96±0.32	2.74±0.35	2.20±0.4	2.17±0.63

The data represent the average and standard deviation (±SD) of three independent experiments. Statistical analysis: No significant differences among the isolates were observed

[a] Esmeraldo has deletions in *ND4* and *ND5*

supported by succinate (~22 and 26% higher for VL10 and FAMEMA strains, respectively). The addition of ADP to the preparations caused an increase in respiratory rates (state 3), whereas oligomycin led to a decrease in oxygen consumption due to ATP synthase inhibition (state 4). RCR were ~2 for the five isolates in the presence of complex I or II substrates. The data indicate that mutations in complex I genes do not affect coupling of oxidative phosphorylation with respiration.

Since RCRs were not higher in the presence of NADH-generating substrates, the data also suggest that complex I is non-functional or has a low activity and NADH generated by pyruvate/malate could be oxidized by other enzymatic pathways. As stated above, a NADH-dependent fumarate reductase (FRD) has been implicated in the oxidation of mitochondrial NADH and generation of succinate in trypanosomatids (Boveris et al. 1986; Besteiro et al. 2002; Coustou et al. 2005; Coustou et al. 2006). In order to test this hypothesis, the same experiments described above were repeated in the presence of the complex II inhibitor malonate (10 mM). Two isolates were chosen, one with no deletions in complex I genes (CL Brener) and another with a *ND7* deletion (VL10). As can be seen in Table 3, the level of respiratory inhibition by malonate and the RCR when pyruvate/malate were used to support respiration was approximately 45% of control in both isolates. Slightly higher levels of RCR inhibition were observed when succinate was used. Malonate promoted an inhibition of approximately 45% in state 3 respiratory rates and 50% in RCRs for both strains respiring on succinate. The similar inhibition levels promoted by malonate with either substrate support the notion that a significant part of

Table 3 Oxygen consumption rates and respiratory control ratios in the presence of complex I or complex II substrates with or without the addition of malonate

	CL Brener (Wt *ND7*)			VL10 (Δ *ND7*)		
	Malonate (−)	Malonate (+)	Inhibition (%)	Malonate (−)	Malonate (+)	Inhibition (%)
Piruvate/malate						
Respiratory rates (nmols O_2 . mg cell protein^{-1} . min^{-1})						
State 3	4.33±0.4	2.04±0.3	47.4±6.7	3.95±0.4	1.69±0.01	43.0±3.5
Respiratory control ratio (State 3/State 4)						
	2.38±0.4	1.14±0.1	47.9±1.1	2.39±0.3	1.08±0.1	46.0±6.5
Succinate						
Respiratory rates (nmols O_2 . mg cell protein^{-1} . min^{-1})						
State 3	4.12±0.5	1.59±0.1	39.2±4.8	4.22±0.5	1.98±0.3	48.2±1.5
Respiratory control ratio (State3/State 4)						
	2.3±0.6	1.16±0.1	52.6±14	2.2±0.4	1.11±0.1	51±6.7

The data represent the average and standard deviation (±SD) of three independent experiments. Statistical analysis: No significant differences among the isolates were observed

NADH is oxidized by mitochondrial FRD (Denicola-Seoane et al. 1992).

Mitochondrial membrane potentials ($\Delta\Psi$)

$\Delta\Psi$ were estimated by flow cytometry in the presence of DiOC6(3), a cationic lipophylic fluorescent compound capable of diffusing into cells and concentrating preferentially into mitochondria (Srivastava et al 1997; Campos et al 2004). $\Delta\Psi$ was determined in the different isolates to evaluate whether mitochondrial gene deletions could promote alterations in this parameter (Fig. 2). Among the isolates, 115 had the highest and Esmeraldo and FAMEMA the lowest relative change in probe fluorescence. As observed with respiratory measurements, no correlation could be established between $\Delta\Psi$ and *ND7*, *ND4* or *ND5* deletions.

Mitochondrial hydrogen peroxide formation

Generation of ROS in the mitochondria is a continuous and physiological event. Through monoelectronic reduction of O_2 at complex I, II and III, the superoxide radical anion ($O_2^{\bullet-}$) can be generated (reviewed by Vercesi et al. 2006; Kowaltowski et al. 2009). This ROS is the precursor of hydrogen peroxide (H_2O_2) and the hydroxyl radical ($OH^{\bullet}$) (Vercesi et al. 2006). An important source of mitochondrial ROS is reverse electron transfer, in which electrons from succinate are transported through ubiquinone to complex I, where they generate $O_2^{\bullet-}$ (Kowaltowski et al. 2009). Mitochondrial H_2O_2 formation induced by different substrates in digitonin–permeabilized epimastigotes was determined using Amplex red and HRP as a probe (Fig. 3a and b). Significant differences were observed in Esmeraldo, 115 and VL10 isolates when complex I or complex II substrates were used. However, no correlation could be established between the amount of H_2O_2 produced and gene deletions, demonstrating that these mutations are not important to oxidant production state. We observed that the lowest H_2O_2 release level was detected in CL Brener and the highest, in the 115 strain. Since we could not attribute the differences in ROS release to alterations in complex I subunits, we measured NAD(P) levels in the two isolates.

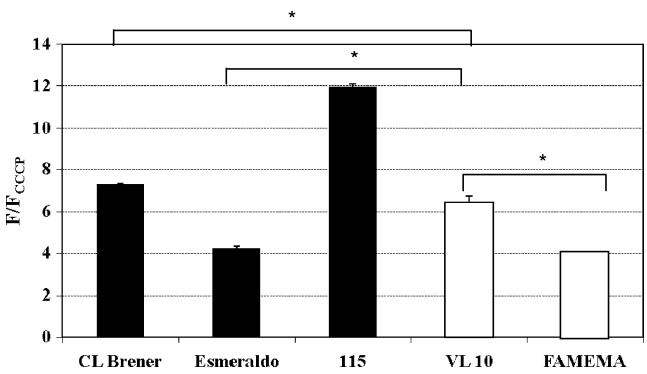

Fig. 2 Mitochondrial membrane potential estimation in intact cells. Epimastigotes were incubated in standard reaction medium in the presence of the fluorescent compound $DiOC_6(3)$. The F/F_{CCCP} ratio was used to estimate changes in $\Delta\Psi$, where F is the mean fluorescence intensity of $DiOC_6(3)$ (F max) and F_{CCCP} is the mean fluorescence in the presence of the uncoupler CCCP (F min). The values presented are averages and standard errors from six independent experiments performed in duplicates. Isolates: Black (Wt *ND7*); white (Δ *ND7*). *Statistical analysis*: * $p > 0.05$

NAD(P) levels

Total, oxidized and reduced NAD(P) levels in the CL Brener and 115 strains were determined fluorimetrically (Fig. 4) under the same reaction conditions used for the measurement of mitochondrial H_2O_2 release in the presence of complex I and II substrates. In the presence of complex I substrates, we observed that the 115 strain displayed a significantly larger quantity of total NAD and NAD^+ than CL Brener (Fig. 4a and b), and that CL Brener NAD levels were maintained in a more reduced state relative to 115 (Fig. 4c). Furthermore, NADH reduction through reverse electron transport in the presence of succinate as a substrate was higher in CL Brener (Fig. 4d). These results suggest that enhanced H_2O_2 release levels in 115 are related to higher levels of total NAD in these mitochondria, and not to enhanced NADH reduction or reverse electron transfer (Turrens 2003; Liu et al. 2002).

Susceptibility to exogenous hydrogen peroxide

Our determinations of mitochondrial ROS release showed substantial differences in oxidant generation among the strains. In order to evaluate if there were also significant changes in the ability to remove ROS, we tested the susceptibility of epimastigotes to exogenously-added H_2O_2, by determining the H_2O_2 concentration that inhibits 50% parasite proliferation (IC_{50}). As seen in Fig. 3c, VL10 and FAMEMA were slightly more susceptible to H_2O_2 treatment, but this difference was not significant (~15%). Thus, growth of all the isolates was equally susceptible to inhibition by H_2O_2, suggesting no gross changes in the levels of intracellular antioxidants.

Maximum NAD(P)H production in the isolates

In view of the results on H_2O_2 susceptibility, we decided to measure the NADPH levels produced by the PPP, since one of the major roles of this pathway is to produce this reduced coenzyme, fundamental in the unique trypanothione-dependent antioxidant system present in this parasite (Mielniczki-Pereira et al. 2007). In fact, trypanothione, an

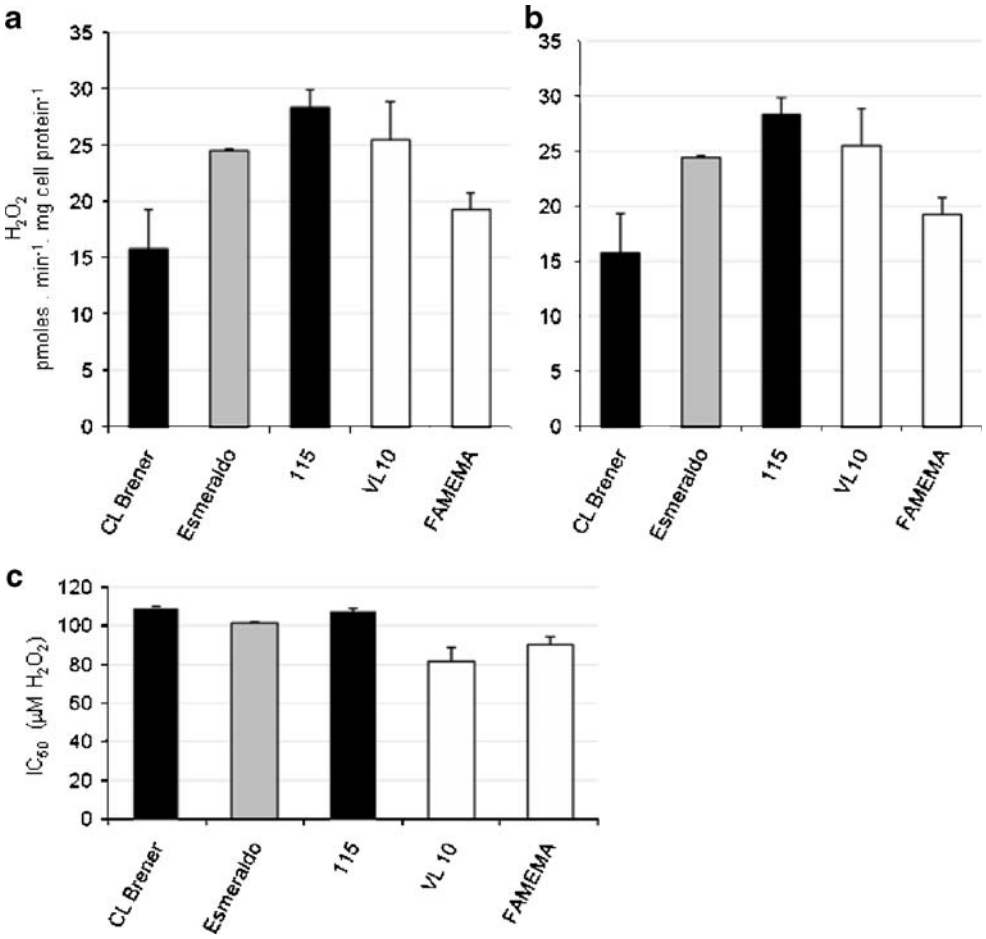

Fig. 3 Hydrogen peroxide production and susceptibility. Mitochondrial H_2O_2 production (Panels **a** and **b**). Digitonin-permeabilized epimastigotes were incubated in SRM with 5 mM pyruvate/5 mM malate (Panel **a**) or 5 mM succinate (Panel **b**) as respiratory substrates. The reaction was initiated by the addition of 50 μM Amplex red and 1 U/mL HRP. Susceptibility of *T. cruzi* isolates to exogenous H_2O_2 (Panel **c**). Epimastigotes were incubated with different H_2O_2 concentrations. IC_{50} corresponds to the H_2O_2 concentration that promotes 50% inhibition of parasite proliferation. Data represent the average and standard deviation of three independent experiments. Isolates: Black (Wt genes); white (Δ *ND7*); grey (Δ *ND4* and *ND5*)

unusual form of glutathione containing two molecules of glutathione joined by a spermidine linker, is reduced by trypanothione reductase using NADPH. As shown in Fig. 5, significant differences were observed among the isolates, but no correlation with ROS generation could be established.

Discussion

In trypanosomatids the involvement of complex I in NADH oxidation has been debated over the years (reviewed by Cazzulo 1994; Bringaud et al. 2006; Opperdoes and Michels 2008). In this study we employed natural mutants of *T. cruzi* bearing large deletions in complex I *genes ND4* and *ND7*, and frame-shift mutations in *ND5*, coding for transmembrane subunits (*ND4* and *ND5*) and a matrix protruding subunit (*ND7*), to investigate the functionality of this complex. All mutations produce truncated products that most certainly should impair the function of the corresponding components. Structural and functional alterations in complex I have been implicated in numerous human diseases, such as Parkinson's disease, Alzheimer's disease, as well aging and apoptosis (reviewed by Lazarou et al. 2007). In *Zea mays* a mutation in *ND4* impairs complex I assembly and plant growth (Yamato and Newton 1999), whereas a deletion in *nd7* originates fragile *Nicotiana sylvestris* plants (Pineau et al. 2005). On the other hand, mutations in *T. cruzi* complex I subunits do not affect the parasite biology, since mutant strains are abundant in nature and pathogenic to humans (Carranza et al. 2009). In contrast, RNAi silencing of expression of subunits of the F0F1-ATP synthase complex drastically impairs the viability of *T. brucei* procyclic forms (Zíková et al. 2009).

Comparative analysis of mitochondrial bioenergetics of Wt and mutant parasites showed no significant differences in oxygen consumption or RCR in the presence of NADH-linked mitochondrial substrates or $FADH_2$-generating succinate. Although differences in the mitochondrial membrane potentials were observed among the isolates, they were not associated to *ND* mutated genes. Taken together, these data indicate that either complex I has a low activity or, less probably, that complex I mutations do not affect mitochondrial respiration and coupling of respiration with oxidative phosphorylation. Interestingly, a series of mutations in the 49 kDa protein (homologous to ND7) of the yeast *Yarrowia lipolytica* decreased or abolished ubiquinone reductase activity (Kashani-Poor et al. 2001).

In trypanosomatids, the oxidation of mitochondrial NADH has been attributed to FRD, which generates

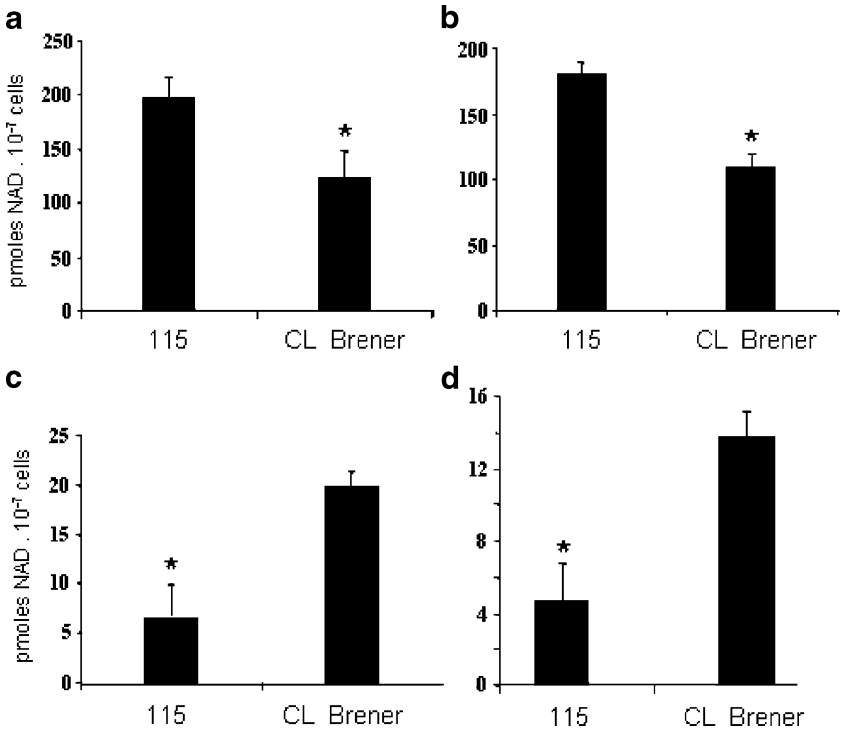

Fig. 4 NAD(P) levels in the 115 and CL Brener strains in the presence of complex I substrates (Panels **a**, **b** and **c**) and succinate (Panel **d**). Total NAD (Panel **a**); total NAD^+ (Panel **b**) and total NADH (Panels **c** and **d**). The data represent the average and standard deviation of three independent experiments. *Statistical analysis*:*$p > 0.05$

succinate from fumarate (Boveris et al. 1986; Besteiro et al. 2002; Coustou et al. 2005; Turrens 1989). Here, we confirmed such an indication by verifying that malonate, an inhibitor of complex II, impaired oxygen consumption and RCR supported by either complex I and II substrates to the same extent. On the other hand, the observed inhibition was approximately 50%, employing malonate at 10 mM, a concentration used to inhibit complex II function in trypanosomatids (Turrens 1989; Coustou et al. 2008). Yet, in those studies the inhibition extent promoted by 10 mM malonate was not reported. Since the malonate concentration used in the present study is in vast excess to that used in other eukaryotes (Maciel et al. 2004), it is possible that the inhibition constant of this compound in trypanosomatids is much higher than that of other organisms.

Benznidazole has been reported to be an inhibitor of partially purified FRD in *T. cruzi* and *T. brucei* (Turrens et al. 1996). To further assess the role of mitochondrial FRD in the oxidation of NADH, we incubated digitonin-permeabilized epimastigotes with respiratory substrates and 50 μM benznidazole. Under this condition, RCRs dropped to ~1.3 with either complex I or II substrates, as compared to the RCR values of ~2 in the absence of the inhibitor (data not shown). This observation suggests that benznidazole has effects on mitochondrial bioenergetics unrelated to FRD inhibition, which may preclude its use in systems involving more than the isolated enzymatic activity.

The ~50% RCR inhibition promoted by malonate when pyruvate/malate were used to support respiration suggests that besides mitochondrial FRD, a fraction of NADH may be oxidized by complex I or by alternative enzymes. This could be the case of a mitochondrial rotenone-insensitive NADH-dehydrogenase (a non-proton translocating NADH-ubiquinone oxidoreductase) described in *T. brucei* (Fang and Beattie 2002). Although a homologous activity has not been reported in *T. cruzi*, the search for similarities using the *T. brucei* enzyme as a query (GenBank accession no. **AY125472**) revealed two sequences in CL Brener (GenBank accession nos. **XM_807104** and **XM_805934**) that showed 67% identity. Since these enzymes do not have a counterpart in the mammalian host, they deserve future attention. Besides that, another possibility for NADH oxidation could be through a nicotinamide nucleotide

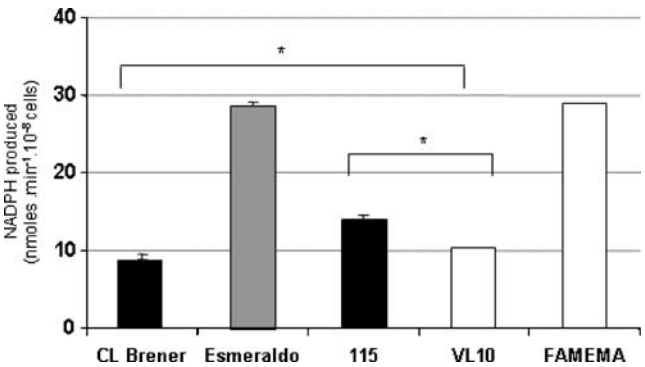

Fig. 5 NADPH production by the pentose phosphate pathway. Epimastigotes were incubated in the medium described in Materials and methods and $NADP^+$ reduction was monitored at 340 nm. Isolates: Black (Wt genes); white (Δ *ND7*); grey (Δ *ND4* and *ND5)*. Statistical analysis: *$p > 0.05$

transhydrogenase, as proposed to occur in mitochondrial pathologies during aging (Olgun 2008). However, such an enzyme has not been identified in *T. cruzi*. Our data and the evidence of alternative pathways for NADH oxidation in trypanosomatids support the suggestion that complex I has no or limited functionality in this process.

In the present study we also formulated the hypothesis that structural alterations of complex I could induce changes in ROS production. In fact, ROS release from complex I can occur both from electrons originating in NADH (forward electron leakage) and from electrons originating from succinate (reverse electron leakage) (Turrens 2003). Significant differences among the strains in mitochondrial H_2O_2 levels induced by different substrates were observed. However, no relationship with the mutated genes was established. The variations seem to be strain-specific and further illustrate the biological and biochemical diversity of *T. cruzi* populations (reviewed by Campbell et al. 2004). The most significant differences in peroxide production were observed in the CL Brener and 115 strains, both displaying Wt *ND* genes. This prompted us to evaluate the NAD(P)H levels in these cells since NADH is the main electron source for ROS generation in most mitochondria. The higher levels of H_2O_2 release observed in the mitochondrion of the 115 isolate cannot be ascribed to a more reduced NADH pool, but may be related to a higher availability of total NAD, as well as to lower respiratory rates and high $\Delta\Psi$ observed in state 4 for this strain. These may provide respiratory chain intermediates with more electrons, leading to higher electron leakage rates.

Even though differences were observed in mitochondrial H_2O_2 generation among the strains, the growth of all the isolates was equally susceptible to exogenously-added H_2O_2, suggesting that the levels of intracellular antioxidants involved in the removal of H_2O_2 may be similar in these cells. In fact, differences in H_2O_2 susceptibility have been ascribed to the presence of different levels of tryparedoxin peroxidase, analogous to glutathione peroxidase present in other eukaryotes (Mielniczki-Pereira et al. 2007). Interestingly, we observed that the levels of NADPH produced by the strains were considerably different, indicating that PPP activity is not a pathway limiting the resistance to oxidative stress generated by H_2O_2 (Maugeri and Cazzulo 2004).

Taken together, our data indicate that alterations in complex I subunits do not correlate with ROS production or NADH oxidation in *T. cruzi* strains. It could be argued that this conclusion is only valid for the *in vitro* cultured epimastigotes grown in a glucose-rich medium. Under this condition, ATP production would be obtained mainly by substrate level phosphorylation. Such would also be the case of the mammalian bloodstream trypomastigotes (Cazzulo 1994). On the other hand, for the insect-stage forms and intracellular amastigotes, which rely on amino acids catabolism, oxidative phosphorylation becomes essential (reviewed by (Cazzulo 1994; Bringaud et al. 2006). Since *ND* gene deletions are a permanent character of the mutants, our results strongly suggest that complex I is non-functional in either parasite stage.

In the proposed model for trypanosomatid complex I four integral membrane subunits involved in the vectorial translocation of protons are missing (Opperdoes and Michels 2008). Accordingly, it appears that complex I is not involved in energy transduction. Interestingly, mitochondria of *Saccharomyces cerevisiae* have a particular type of NADH dehydrogenase, distinct from complex I of the other eukaryotes, that does not contain a proton translocation site and is insensitive to rotenone (Yagi et al. 2006 and cited references).

Provided that complex I is non-functional in NADH oxidation in trypanosomatids, and taking into consideration that it is not involved in energy transduction, one could ask why these unneeded genes persist. A possible hypothesis to maintain complex I would be its cooperation in the formation of respiratory super-complexes that would allow a more efficient electron transfer. The role of these super-complexes is not clear but it appears to involve substrate channeling, as well as complex stability (Lazarou et al. 2007). In mammalian, as well as plant mitochondria a supercomplex consisting of complex I and III has been found (Vonck and Schäfer 2008). It will be of interest to investigate such an aspect in *T. cruzi*. Altogether, it is clear that trypanosomatids present significant differences in energy metabolism relative to mammalian cells that warrant more in depth investigation.

Acknowledgements We thank Marcelo N. Silva, Camille C. Caldeira da Silva and Luis Henrique Gonzaga Ribeiro for technical assistance. We are indebted to Nancy R. Sturm for insightful suggestions. This work was supported by grants of Fundação de Amparo à Pesquisa do Estado de São Paulo (FAPESP), Ministério de Ciência e Tecnologia/Conselho Nacional de Desenvolvimento Científico e Tecnológico/Ministério da Saúde (MCT/CNPq/MS-SCTIE-DECIT- Edital de Doenças Negligenciadas) (BZ) and INCT de Processos Redox em Biomedicina (AJK). JCC was recipient of a graduation fellowship from the Universidad del Tolima (Ibagué, Colombia) and Instituto Colombiano Francisco José de Caldas (COLCIENCIAS).

References

Baptista C, Vêncio R, Abdala S, Carranza J, Westerberger S, Silva M, de B Pereira C, Galvão L, Gontijo E, Chiari E, Sturm N, Zingales B (2006) Mol Biochem Parasitol 150:236–248

Besteiro S, Biran M, Biteau N, Coustou V, Baltz T, Canioni P, Bringaud F (2002) J Biol Chem 277:38001–38012

Boveris A, Hertig C, Turrens J (1986) Mol Biochem Parasitol 19:163–169

Bradford M (1976) Anal Biochem 72:248–254

Bringaud F, Riviere L, Coustou V (2006) Mol Biochem Parasitol 149:1–9
Campbell DA, Westenberger SJ, Sturm NR (2004) Curr Mol Med 4:549–562
Campos C, Degasperia GR, Pacífico D, Albericia L, Carreira R, Guimarães F, Castilho R, Vercesi A (2004) Biochem Pharmacol 68:2197–2206
Cannata J, Cazzulo J (1984) Comp Biochem Physiol B 79:297–308
Carranza JC, Valadares HMS, D'Ávila DA, Baptista RP, Moreno M, Galvão LMC, Chiari E, Sturm NR, Gontijo ED, Macedo AM, Zingales B (2009) Int J Parasitol 39:963–973
Castellani O, Ribeiro LV, Fernandes JF (1967) J Protozool 4:447–451
Cazzulo J (1994) J Bioenerg Biomembranes 26:157–165
Coustou V, Besteiro S, Riviere L, Biran M, Biteau N, Franconi J, Boshart M, Baltz T, Bringaud F (2005) J Biol Chem 280:16559–16570
Coustou V, Biran M, Besteiro S, Riviere L, Baltz T, Franconi F, Bringaud F (2006) J Biol Chem 281:26832–26846
Coustou V, Biran M, Breton M, Guegan F, Rivière L, Plazolles N, Nolan D, Barrett MP, Franconi JM, Bringaud F (2008) J Biol Chem 283:16342–16354
Denicola-Seoane A, Rubbo H, Prodanov E, Turrens J (1992) Mol Biochem Parasitol 54:43–50
Fang J, Beattie D (2002) Biochemistry 41:3065–3072
Kashani-Poor N, Zwicker K, Kerscher S, Brandt U (2001) J Biol Chem 276:24082-24087
Kowaltowski AJ, Fenton G, Fiskum GZ (2004) Free Radical Biology & Medicine 37:1845–1853
Kowaltowski AJ, de Souza-Pinto NC, Castilho RF, Vercesi AE (2009) Free Radic Biol Med May 7. doi:10.1016/j.freeradbiomed.2009.05.004
Lazarou M, Mckenzie M, Ohtake A, Thorburn D, Ryan M (2007) Mol Cell Biol 27:4228–4237
Liu Y, Fiskum G, Schubert D (2002) J Neurochem 80:780–787
Maciel EN, Kowaltowski AJ, Schwalm FD, Rodrigues JM, Souza DO, Vercesi A, Wajner M, Castilho RF (2004) J Neurochem 90:1025–1035
Maugeri D, Cazzulo J (2004) FEMS Microbiol 234:117–223
Mayevsky A, Rogatsky G (2007) Am J Physiol Cell Physiol 292:615–640
Mielniczki-Pereira A, Chiavegatto C, López J, Colli W, Alves MJM, Gadelha F (2007) Acta Trop 101:54–60
Olgun A (2008) Biogerontology Oct 19. doi:10.1007/s10522-008-9190-2
Opperdoes F, Michels P (2008) Trends Parasitol 24:310–317
Pineau B, Mathieu C, Gérard-Hirne C, De Paepe R, Chétrit P (2005) J Biol Chem 280:25994–26001
Simpson L, Neckelmann N, de La Cruz VF, Simpson AM, Feagin JE, Jasmer DP, Stuart JE (1987) J Biol Chem 262:6182–6196
Srivastava IK, Rottenberg H, Vaidya AB (1997) J Biol Chem 272:3961–3966
Stuart K, Panigrahi AK, Schnaufer A, Drozdz M, Clayton C, Salavati R (2002) Philos Trans R Soc Lond Biol Sci 357:71–79
Turrens J (1989) Biochem J 259:363–368
Turrens J (2003) J Physiol 552:335–344
Turrens J, Watts B, Zhong L, Docampo R (1996) Mol Biochem Parasitol 82:125–129
Vercesi A, Bernardes C, Hoffmann M, Gadelha F, Docampo R (1991) J Biol Chem 266:14431–14444
Vercesi A, Kowaltowski AJ, Oliveira H, Castilho RF (2006) Frontiers in Bioscience 11:2554–2564
Vonck J, Schäfer E (2008) Biochim Biophys Acta 1793:117–124
Westenberger S, Cerqueira G, El-Sayed N, Zingales B, Campbell D, Sturm N (2006) BMC Genomics 7:1–18
Yagi T, Seo B, Nakamaru-Ogiso E, Marella M, Barber-Singh J, Yamashita T, Kao M, Matsuno-Yagi A (2006) Rejuvenation Res 9:191–197
Yamato K, Newton K (1999) J Hered 90:369–373
Zhou M, Diwu Z, Panchuk-Voloshina N, Haugland R (1997) Anal Biochem 253:162–168
Zíková A, Schnaufer A, Dalley RA, Panigrahi AK, Stuart KD (2009) PLoS Pathog May 5:e1000436